ELSEVIER

Journal of Pharmaceutical and Biomedical Analysis
23 (2000) 927–937

JOURNAL OF
PHARMACEUTICAL
AND BIOMEDICAL
ANALYSIS

www.elsevier.com/locate/jpba

Identification of autoxidation and photodegradation products of ethynylestradiol by on-line HPLC–NMR and HPLC–MS

Brigitte E. Segmuller, Barbara L. Armstrong, Richard Dunphy, Alan R. Oyler *

The R.W. Johnson Pharmaceutical Research Institute, Room J-214, 1000 Route 202 South, Raritan, NJ 08869-0602, USA

Received 22 February 2000; received in revised form 26 May 2000; accepted 26 May 2000

Abstract

HPLC–NMR, HPLC–MS, and HPLC–UV were used to characterize the predominant solution autoxidation and photodegradation products of ethynylestradiol (**1**). A hydroperoxide (**2**) and a series of isomeric dimeric oxidation products (**3**–**7**), were identified.

Keywords: Ethynylestradiol; Estrogen; HPLC–MS; HPLC–NMR; Autoxidation; Photodegradation

1. Introduction

Ethynylestradiol (**1**;(17α)-19-norpregna-1,3,5-(10)-trien-20-yne-3,17-diol) is a synthetic estrogenic steroid that has therapeutic uses (e.g. oral contraception). The degradation chemistry of this compound has not been extensively studied. The autoxidation of **1** in the solid state was reported to give a product mixture that included Δ^6-dehydroethynylestradiol, 6-ketoethynylestradiol, and 6-hydroxyethynylestradiol [1]. Photodegradation in the solid state was also observed but products were not identified [2]. The photosensitized degradation of **1** in solution gave a hydroperoxide derivative [3]. This report describes a further investigation of the autoxidation and photodegradation chemistry of ethynylestradiol in solution.

The structural elucidation of individual compounds in complex mixtures, such as those derived from the degradation of steroids, has traditionally involved the time-consuming isolation of each compound to be addressed. Recently, an alternative approach that does not require isolation has gained favor [4–19]. This approach is based upon a combination of multiple on-line hyphenated techniques including HPLC–NMR and has been used for structural assignments in areas such as drug impurities [7,11,17,19], drug degradation products [14], drug metabolites [13,18], and natural product chemistry

* Corresponding author. Tel.: +1-908-7044430; fax: +1-908-7041612.

E-mail address: aoyler@prius.jnj.com (A.R. Oyler).

0731-7085/00/$ - see front matter
PII: S0731-7085(00)00363-0

[4,5,7,9,10,12,15]. Separate HPLC–MS and HPLC–NMR analyses are often performed but directly coupled HPLC–NMR–MS is an alternative. Practical considerations for the use of the directly coupled technique have been presented [16]. This study used the on-line approach with separate HPLC–UV–MS and HPLC–UV–NMR experiments.

2. Materials and methods

2.1. Reagents and chemicals

Ethynylestradiol was obtained from the United States Pharmacopeia (USP, Rockville, MD) and Diosynth (Oss, Netherlands). Trifluoroacetic acid and HPLC grade water were from J.T. Baker (Phillipsburg, NJ). Acetonitrile was obtained from Burdick and Jackson (Muskegon, MI) or EM Science (Gibbstown, NJ; used exclusively for the NMR studies). Deuterated acetonitrile was obtained from Isotec (Miamisburg, OH). Deuterium oxide (99.9%) was from Cambridge Isotope Laboratories (Andover, MA). 2,2′-Azobisisobutyronitrile (AIBN), propylene glycol, and ammonium acetate were obtained from Aldrich (Milwaukee, WI). The oxygen was extra dry grade from Air Products (Allentown, PA).

2.2. Autoxidation reaction procedure

In a typical reaction, ethynylestradiol (1.17 g, 3.93×10^{-3} mol) and AIBN (3.2 g, 1.97×10^{-2} mol) were placed into a 25-ml volumetric flask and the flask was filled to the mark with acetonitrile (concentration of **1** = 46.8 mg/ml). Approximately 10 ml of this solution was set aside (initial sample). The remaining solution was transferred to a scintillation vial which was capped loosely with aluminum foil and placed into a 450-ml glass-lined stainless-steel reactor (Parr Instruments, Moline, IL). The reactor was pressurized with oxygen (300 psi) and then placed into an oven at 50 ± 1°C for 6 h. The vial was removed from the reactor, capped, and placed into a refrigerator prior to HPLC analysis.

A second reaction was conducted in a similar manner with a 10-fold more dilute solution prepared by adding ethynylestradiol (206.89 mg, 6.99×10^{-4} mol) and AIBN (0.57 g, 3.50×10^{-3} mol) to a 50-ml volumetric flask and diluting to the mark with acetonitrile (concentration of **1** = 4.1 mg/ml).

2.3. Photodegradation reaction procedure

Ethynylestradiol (215.88 mg) was placed into a 50-ml volumetric flask and the flask was filled to the mark with acetonitrile (concentration of **1** = 4.3 mg/ml). Approximately 3 ml of this solution was set aside (initial sample). The remaining solution was transferred to a quartz vessel ($8.5 \times 13 \times 3.2$ cm; liquid height was approximately 4 mm). The vessel was tightly capped and placed into a Suntest™ CPS light box (Atlas, Chicago, IL) that was equipped with a xenon lamp and a window glass filter (310 nm cutoff). The bottom plate temperature was ca. 34°C and the chamber temperature was ca. 42°C. The irradiance was 765 W/m^2. After 8.7 h, the reaction solution was removed and stored in a refrigerator prior to HPLC analysis.

2.4. HPLC–UV procedure

Gradient reversed-phase HPLC was conducted on a Hewlett–Packard (Wilmington, DE) Series 1100 instrument at 50°C with a 250×4.6 mm Luna™ C18(2) column (5-μm particles; Phenomenex, Torrance, CA). The flow rate was 1.2 ml/min. Mobile phase A was water with 0.05% (v/v; 4 mM) trifluoroacetic acid. Mobile phase B was acetonitrile with 0.05% (v/v; 4 mM) trifluoroacetic acid. The solvent program began at A:B (95:5, v/v), proceeded to A:B (25:75, v/v) over 70 min, and then to A:B (0:100, v/v) over 15 min. The primary detection wavelength was 220 nm and UV spectra of each peak were collected. USP reference standard solutions of **1** were prepared at concentrations of ca. 0.3 mg/ml. Reaction solutions were diluted as required to ca. 0.3 mg/ml. The injection volume was 25 μl. The trifluoroacetic acid was added to the mobile phases to suppress formation of dimeric oxidation products

(**3**–**7**) on the HPLC column. Peaks corresponding to these compounds sometimes appeared during the reversed-phase HPLC analysis of some samples of **1**.

2.5. HPLC–MS procedure

Mass spectral data were obtained with an HPLC–MS instrument that consisted of a Perkin–Elmer (Norwalk, CT) Series 200 HPLC coupled to a Finnigan MAT900 mass spectrometer (Bremen, GR).

Positive ion mass spectral data were obtained in the atmospheric chemical ionization (APCI) mode. The vaporizer temperature was 450°C, the discharge current was 4 μA, and the scanned m/z range was 150–1000 Da. Nitrogen was used as the sheath gas (40 psi) and the auxiliary gas (20 arbitrary units). The typical HPLC conditions were described above. High resolution mass spectral data were acquired by electric voltage scan in the high resolution centroid mode. A mass range of 550–625 Da was scanned at a rate of 9 s per decade (0.5-s cycle time). The spectrometer resolution at m/z 558 was 3400 (10% valley definition). A polypropylene glycol reference solution was added after the column by a syringe pump (10 μl/min). This reference solution contained 1×10^{-6} M polypropylene glycol (average molecular weight = 425) and 10-mM ammonium acetate in water. In each mass spectral scan, the ions of interest were bracketed by ions of the reference compound. The data were processed with Finnigan ICIS software and the exact mass reported for each compound was the average of a minimum of 15 separate measurements.

Negative ion mass spectral data were obtained in the electrospray (ESI) mode. The electrospray voltage was 2.5 keV. The scanned m/z range was 150–1000 Da. Sheath and auxiliary gas conditions were the same as for the APCI analysis. The HPLC conditions were the same as those described above except that the trifluoroacetic acid was omitted. The numbers of exchangeable protons were determined (in the negative ionization mode) in HPLC–MS experiments with D_2O rather than H_2O in mobile phase A.

2.6. HPLC–NMR procedure

NMR data were obtained with a Varian (Walnut Creek, CA) HPLC system coupled to a Varian UnityPlus 500 NMR instrument (500 MHz) or a Varian UnityInova 500 NMR instrument (500 MHz). The NMR instruments were fitted with a Varian flow probe with a 60-μl flow cell. The HPLC conditions were the same as those described above except for the use of deuterated solvents in the mobile phases. The majority of the experiments were conducted with D_2O/CH_3CN but some experiments were conducted with D_2O/CD_3CN. Furthermore, to maximize sensitivity, the injection amount was increased by injecting 50 μl of a 46.8 mg/ml product mixture. Several injections were made to acquire the complete NMR data set. The data were acquired in stopped-flow mode with suppression of the acetonitrile and deuterium oxide signals. The solvent suppression was carried out by using the WET pulse sequence [20]. A composite 90° read pulse was used in all experiments. All free induction decay (FID) data were processed with solvent subtraction for further suppression of the acetonitrile. All spectra were referenced to acetonitrile at 1.95 ppm. One-dimensional proton spectra were acquired for all chromatographic peaks. COSY and NOESY data were acquired for **2**, **3a**, and **6**. NOESY data for **6** were collected with D_2O/CD_3CN in the HPLC mobile phase since useful data were not obtained with D_2O/CH_3CN.

3. Results

3.1. Autoxidation

The autoxidation of ethynylestradiol (**1**) in solution required rigorous conditions. Reactions were conducted in acetonitrile under oxygen (300 psi) at 50°C. 2,2′-Azobisisobutyronitrile (AIBN) was used as a free radical initiator since little reaction occurred in the absence of this initiator. After 6 h, approximately 20–23% of the original ethynylestradiol had degraded (Table 1). The HPLC profiles of the resulting reaction solutions showed numerous products. However, seven

products appeared to predominate (**2**–**7**; Figs. 1 and 2). Reactions conducted with initial ethynylestradiol concentrations of 4.1 and 46.8 mg/ml showed similar profiles (Table 1). Thus an 11-fold variation in the initial ethynylestradiol concentration did not appear to have a major effect upon the levels of the dimeric degradation products (**3**–**7**).

On-line HPLC–NMR, HPLC–MS, and HPLC–UV data were acquired for the autoxidation product mixture (Fig. 2) and used to assign structures to the predominant products (**2**–**7**). Selected data for these products along with the corresponding data for ethynylestradiol are presented in Tables 2 and 3 and Fig. 3. Deuterated solvents were substituted for non-deuterated solvents in the HPLC mobile phase for HPLC–NMR experiments but this substitution did not make a significant difference in the chromatography. Mobile phase with D_2O was also used in one HPLC–MS experiment to determine the number of exchangeable protons in products **3**–**7**. To maximize the quality of the NMR data, the amount of material injected for HPLC–NMR analyses was up to 300-fold more than the amount used for the HPLC–UV analyses. This increased loading caused some slight degradation in the chromatographic separation but not enough to interfere with the collection of NMR data for the individual mixture components.

*3.1.1. Product **2***

The 9-hydroperoxide **2** was identified in the autoxidation product mixture (Fig. 2). The HPLC–UV spectrum of the product was very similar to the HPLC–UV spectrum of **1** and therefore the original aromatic A-ring was intact. High resolution HPLC–MS data supported a structure that consisted of an ethynylestradiol molecule plus two oxygen atoms (Table 2). ^{1}H NMR, COSY, and NOESY data were also collected by HPLC–NMR in the stopped-flow mode (Table 3 and Fig. 3). In the NOESY experiment, an NOE was observed between the H-4 proton and the two H-6 protons. These data indicated that the benzylic C-6 carbon was unaltered (i.e. no oxygens were attached). Furthermore, no NOE was observed between H-1 and an H-11 proton as in the case of **1**. The lack of this NOE indicated that oxygen atoms had been attached to the other benzylic carbon (at C-9) and these atoms eliminated the NOE between the H-1 and H-11 protons. The aromatic signals (between 6.4 and 6.7 ppm) observed for the product were consistent with the reported signals for the aromatic protons of the 9α- and 9β-hydroperoxides of estradiol [21]. The product was therefore assigned as **2**. The stereochemistry at C-9 was not determined.

*3.1.2. Products **3**–**7***

The isomers **3**–**7** were likewise identified in the autoxidation product mixture with similar techniques. The HPLC–UV spectra for all of these products (**3**–**7**) were similar to the HPLC–UV spectrum of **1**, which indicated that the aromatic A-rings were intact. These products gave HPLC–MS spectra that were similar to each other (Table 2). Negative ion HPLC–ESI–MS gave intense $[M–H]^-$ molecular ions at m/z 589 while positive ion HPLC–APCI–MS gave intense $[M+H-$

Table 1
Reaction data[a]

Compound number	**2**	**1**	**3a**	**4**	**3b**	**5**	**6**	**7**
Relative retention time	0.59	1.00	1.25	1.31	1.32	1.35	1.53	1.54
Autoxidation (initial concentration of **1** = 46.8 mg/ml; 6.0 h)[b]	1.0	77	2.7	1.6	1.8	1.8	1.5	1.6
Autoxidation (initial concentration of **1** = 4.1 mg/ml; 6.1 h)[b]	1.0	80	2.4	1.1	1.5	1.3	1.3	1.3
Photodegradation (initial concentration of **1** = 4.3 mg/ml; 8.7 h)[b,c]	0.2	104	0.6	0.4	0.5	0.5	1.0	1.8

[a] Percent of initial concentration (mg/ml) determined by HPLC–UV.
[b] HPLC response factors (weight basis) for products were assumed to be equal to the response factor (weight basis) for **1**.
[c] Some solvent may have evaporated.

Table 2
UV and mass spectral data

Compound number	**1**	**2**	**3a**	**3b**	**4**	**5**	**6**	**7**
Empirical formula	$C_{20}H_{24}O_2$	$C_{20}H_{24}O_4$	$C_{40}H_{46}O_4$	$C_{40}H_{46}O_4$	$C_{40}H_{46}O_4$	$C_{40}H_{46}O_4$	$C_{40}H_{46}O_4$	$C_{40}H_{46}O_4$
HPLC–UV data	λ_{max} 281	λ_{max} 291[a]	λ_{max} 285[a]	λ_{max} 286[a]	λ_{max} 289[a]	λ_{max} 287[a]	λ_{max} 282[a]	λ_{max} 285[a]
(−)-ESI–MS observed $[M–H]^{-}$[b]	295 (100)	NA[c]	589 (100)	589 (100)	589 (100)	589 (100)	589 (100)	589 (100)
(−)-ESI–MS observed $[M'–D]^{-}$[d]	296 (100)	NA	592 (100)	592 (100)	592 (100)	592 (100)	591 (100)	591 (100)
(+)-APCI–MS observed $[M+H]^{+}$[b]	NA	329 (100); 329.177	NA	NA	NA	NA	NA	NA
Calculated $[M+H]^{+}$[b]	297.186	329.175	591.348	591.348	591.348	591.348	591.348	591.348
(+)-APCI–MS observed $[M+H-H_2O]^{+}$[b]	279 (100)	311 (40)	573 (100); 573.337	573 (100); 573.339	573 (100); 573.341	573 (100); 573.338	573 (100); 573.340	573 (100); 573.340
Calculated $[M+H-H_2O]^{+}$	279.170	311.160	573.337	573.337	573.337	573.337	573.337	573.337
(+)-APCI–MS observed $[M+H-2H_2O]^{+}$[b]	NA	293 (78)	NA	NA	NA	NA	NA	NA

[a] UV spectrum was similar to UV spectrum of **1**.
[b] Low resolution (relative intensities); high resolution. Mobile phases with H_2O.
[c] NA, not applicable.
[d] Low resolution. Deuterated mobile phase. The 'M'' indicates that some original hydrogens had been exchanged for deuteriums.

Table 3
NMR spectral data[a]

Compound number	1	2	3a	3b	4	5	6	7
H-1[b]	7.07 (d, 8.7)	6.61 (d, 9)	7.12 (d, 8.4)	7.12 (d, 8.4)	6.79 (s)	7.10 (d, 8.6)	7.12 (d, 8.6)	7.14 (d, 8.5)
H-1′[b]	NA	NA	Same as H-1	Same as H-1	Same as H-1	6.74 (s)	7.02, (d, 8.8)	6.79 (s)
H-2[b]	6.52 (dd, 8.4, 2)	6.48 (dd, 8.7, 3.2)	6.65 (d, 8.6)	6.63 (d, 8.2)	NA	6.63 (d, 8.7)	6.46 (d, 8.7)	6.55 (d, 8.5)
H-2′[b]	NA	NA	Same as H-2	Same as H-2	NA	NA	6.71, (d, 8.7)	NA
H-4[b]	6.47 (d, 2)	6.54 (d, 2.9)	NA	NA	6.56 (s)	NA	6.39 (s)	6.47 (s)
H-4′[b]	NA	NA	NA	NA	Same as H-4	6.56 (s)	NA	6.60 (s)
H-6[b]	2.68 (m)	2.44[c], 2.36 (m)	2.2[c]	ND	2.74 (m)	ND	2.67 (m)	ND
H-6′[b]	NA	NA	Same as H-6	ND	2.74 (m)	ND	2.61 (dd, 17.5, 5.4), 2.34[c]	ND
H-11[b]	α 2.26 (m), β ND	ND	α 2.31–2.34 (m), β 1.36[c]	ND	ND	ND	2.27[c], 1.34[c]	ND
H-11′[b]	NA	ND	Same as H-11	ND	ND	ND	2.32[c], ND	ND
H-18 (H-18′)[b]	0.75 (s)	1.00 (s)	0.75 (s)	0.75 (s)	0.75 (s)	0.75 (s)	0.75 (s)	0.73 (s)[d], 0.75 (s)[d]
H-20 (H-20′)[b]	2.84 (s)	2.89 (s)	2.83 (s)	2.83 (s)	2.82 (s)	2.81 (s)[d], 2.82 (s)[d]	2.81 (s)	2.78 (s)[d], 2.80 (s)[d]

[a] NA, not applicable; ND not determined.
[b] Chemical shifts in ppm. Multiplicities and coupling constants in Hz are shown in parentheses. The estimated error in the coupling constants was ± 0.3 Hz.
[c] Chemical shifts were taken from 2D spectrum due to overlapping peaks.
[d] Individual protons were not assigned to a specific ethynylestradiol moiety.

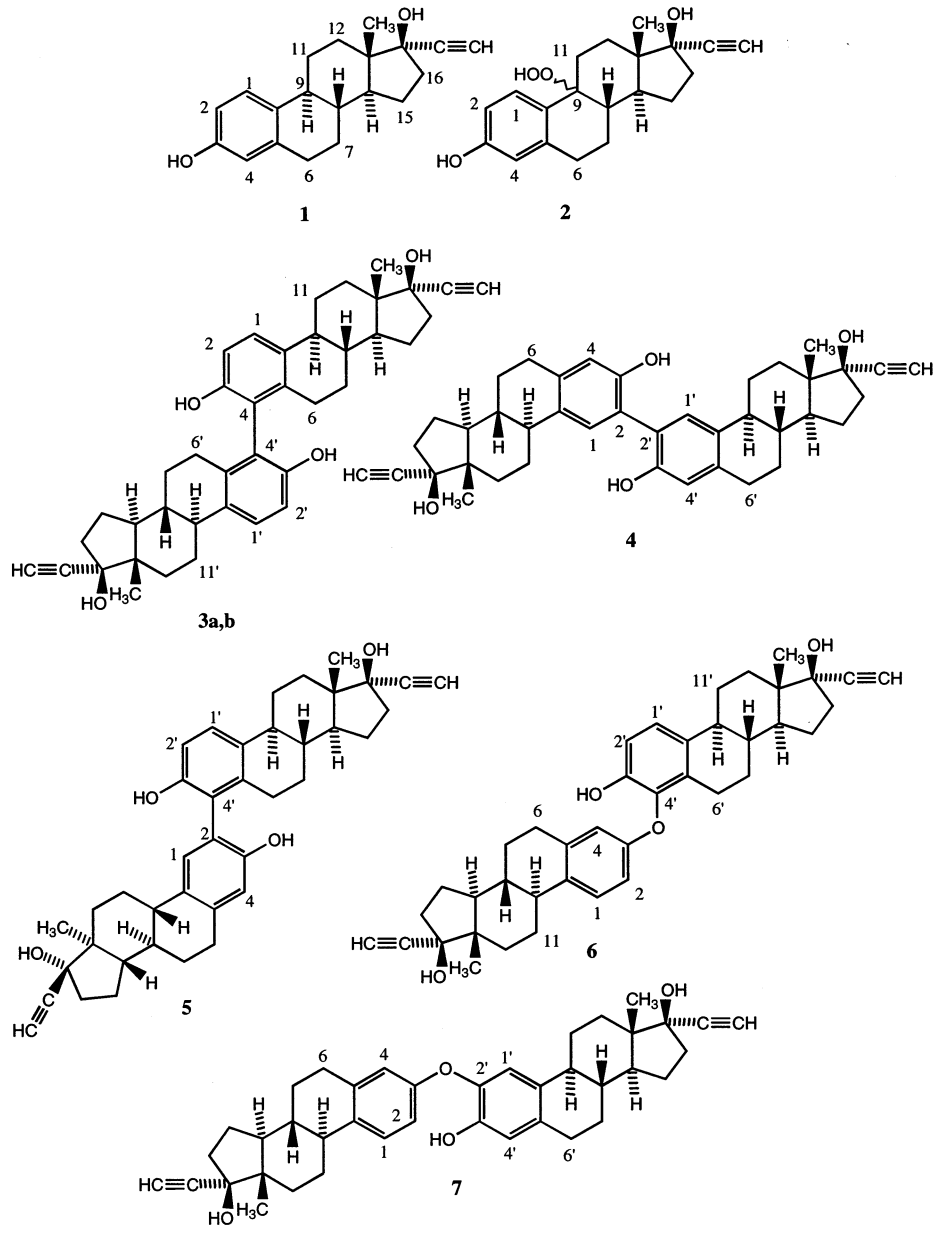

Fig. 1. Structures for compounds.

$H_2O]^+$ ions at m/z 573. For comparison, the parent compound (**1**) gave corresponding intense $[M–H]^-$ molecular ions at m/z 295 in the negative ion HPLC–ESI–MS and intense $[M + H - H_2O]^+$ ions at m/z 279 in the positive ion HPLC–APCI–MS. These data and high resolution data (Table 2) for the individual $[M + H - H_2O]^+$ ions were consistent with the formation of a series of isomers (**3**–**7**) that consisted of two ethynylestradiol moieties less two hydrogen atoms.

Negative ion HPLC–ESI–MS experiments with deuterated mobile phase (i.e. D_2O in place of

H_2O) were used to determine the number of exchangeable protons in each of the dimeric products (**3**–**7**; Table 2). These data were used to differentiate isomers with C–C joining bonds (**2**–**5**) from isomers with C–O joining bonds (**6**–**7**). Ethynylestradiol (**1**) gave intense $[M–H]^-$ molecular ions at m/z 295 with H_2O in the HPLC mobile phase (as noted above) and intense $[M'–D]^-$ molecular ions at m/z 296 with D_2O in the mobile phase (where ‘′’ denotes a molecule with exchanged hydrogens). Presumably, deuterium exchange occurred at the 17-OH and the ArOH groups of **1** in the deuterated HPLC mobile phase and then D^+ was lost in the ionization process to give $[M'–D]^-$ molecular ions. Thus these data showed the presence of two exchangeable protons in **1** (one by the observation of the loss of D^+ and one by the observation of the addition of one deuterium). Likewise, data were collected for the dimeric products (**3**–**7**) in the same two experiments with H_2O and D_2O mobile phases. In H_2O mobile phase, all dimeric products (**3**–**7**) showed $[M–H]^-$ molecular ions at m/z 589 as indicated above. However, in D_2O mobile phase, some products (**3**–**5**) showed $[M'–D]^-$ ions at m/z 592, while other products (**6**–**7**) showed $[M'–D]^-$ ions at m/z 591. By analogy to the interpretation of the mass spectral data for **1**, the number of exchangeable protons on the former products (**3**–**5**) were deduced to be 4 while the number on the latter products (**6**–**7**) were deduced to be only 3.

Finally, the HPLC–NMR data described below were used to determine how the individual ethynylestradiol moieties were joined in these isomers (Fig. 3 and Table 3).

Product **3a** showed only two types of aromatic protons in the ^1H NMR spectrum and these two types of protons were coupled to each other. Thus, there was a doublet at 6.65 ppm ($J = 8.6$ Hz) for the H-2 and H-2′ protons (where ‘′’ indicates an atom on the second ethynylestradiol moiety) and a doublet at 7.12 ppm ($J = 8.4$ Hz) for the H-1 and H-1′ protons (with coupling between the H-1 and H-2 protons and between the H-1′ and H-2′ protons). The H-4 and H-4′ protons were missing. These data suggested that the aromatic rings of the two ethynylestradiol moieties were joined between the C-4 and C-4′

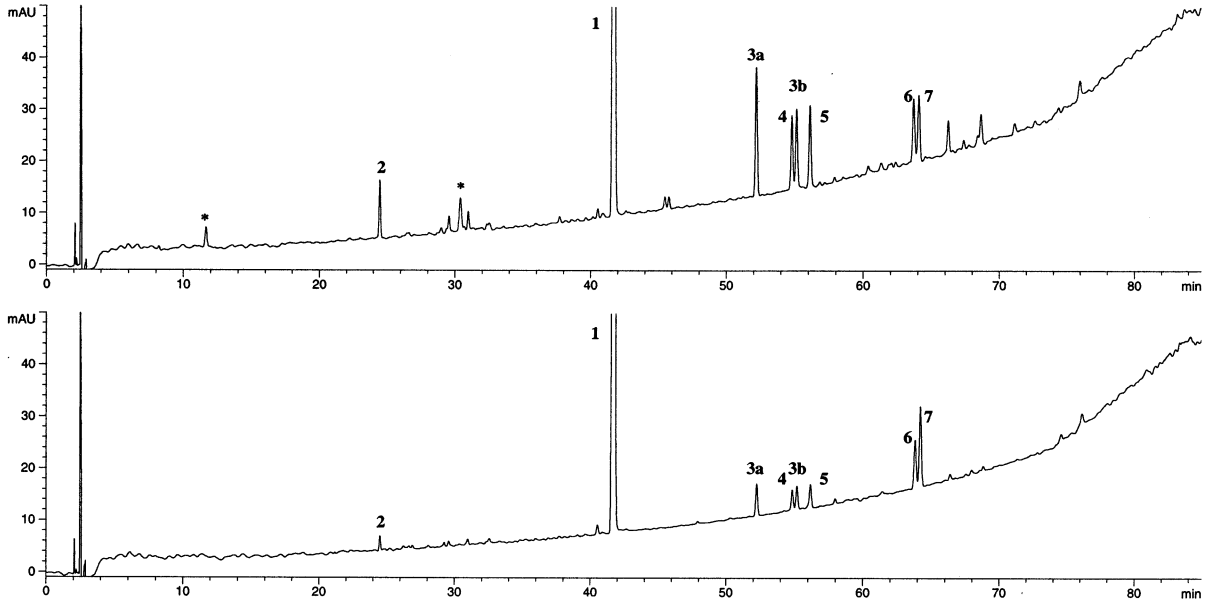

Fig. 2. HPLC–UV chromatograms (220 nm), top, autoxidation product mixture after 6 h (initial concentration of **1** = 46.8 mg/ml). The ‘*’ indicates peaks for AIBN-related species; bottom, photodegradation product mixture after 8.7 h.

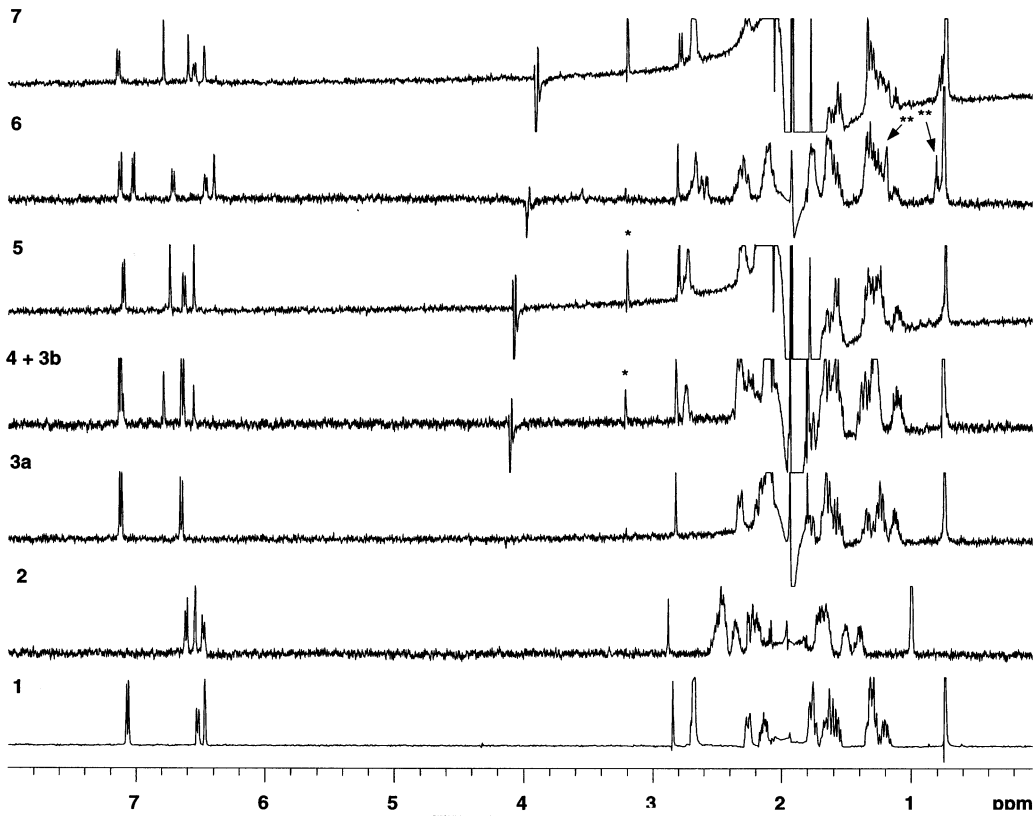

Fig. 3. Stop-flow ^{1}H NMR spectra of **1**–**7** in an autoxidation product mixture after 6 h (initial concentration of **1** = 46.8 mg/ml). The spectrum for **6** was acquired with CD_3CN/D_2O in the mobile phase. The '*' indicates peaks due to methanol. The '**' indicates peaks due to column packing material.

carbons to form the symmetrical biphenyl compound **3a**. This structural assignment was confirmed with COSY and NOESY experiments. In the NOESY experiment, NOE's were observed between the H-1 or H-1′ proton and the corresponding H-11α proton on the same ethynylestradiol moiety. Additionally, NOE's were observed between CH_3 protons and the corresponding H-8, H-15, and H-11β protons on the same ethynylestradiol moiety. With this information, the chemical shift of the H-6 and H-6′ protons could be determined (2.2 ppm). Thus, the H-6 and H-6′ protons were more shielded in the product than the corresponding H-6 protons in ethynylestradiol (2.68 ppm). This shielding was due to the non-planarity of the biphenyl moiety of the molecule which forced the H-6 and H-6′ protons to be over the plane of the opposite aromatic ring. This same effect was reported for some related dimeric phenols [22]. Further evidence for the non-planarity of the aromatic rings was provided by the UV spectrum for **3**. This UV spectrum was similar to the UV spectrum of **1**, which suggested that the interplanar angle between the two aromatic rings was close to 90° [23]. Thus the data for the product were consistent with the assigned structure (**3a**). Furthermore, tetrasubstituted biphenyls such as **3a** are known to have hindered rotation about the carbon–carbon bond joining the two aromatic moieties (atropisomerism) [23]. A second rotamer (rotational isomer) was also observed (**3b**, see below). The absolute stereochemistries about the C-4 to C-4′ carbon–carbon bonds of the individual symmetrical rotamers **3a** and **3b** were not assigned.

Product **3b** nearly coeluted with product **4**, and therefore, a composite ^{1}H NMR spectrum was obtained at the apex of the HPLC–NMR peak. However, NMR data were also acquired across the HPLC–NMR peak to allow the differentiation of NMR signals for **4** from those of **3b**. The ^{1}H NMR spectrum for **3b** showed two doublets in the aromatic region at 6.63 ppm ($J = 8.2$ Hz) and 7.12 ppm ($J = 8.4$ Hz). These data were almost identical to the data obtained for **3a**, and therefore, the structure was assigned as the rotamer **3b**. As noted above, the stereochemistries about the C-4 to C-4′ carbon–carbon bonds of the individual rotamers **3a** and **3b** were not determined.

Product **4** gave two singlets in the aromatic region of the ^{1}H NMR spectrum at 6.56 and 6.79 ppm which were ascribed to the H-4 and H-4′ protons and to the H-1 and H-1′ protons, respectively. These data indicated that the structure of the degradation product was the symmetrical biphenyl isomer **4** which was coupled at the C-2 and C-2′ carbons.

Product **5** showed two doublets and two singlets in the aromatic region of the ^{1}H NMR spectrum. Data collected across the HPLC–NMR peak indicated that this peak represented only one degradation product. The structure was assigned as a non-symmetrical dimeric oxidation product **5** with a bond between the C-2 carbon of one steroid moiety and the C-4′ carbon of the second steroid moiety.

Product **6** showed five signals (four doublets and a singlet) in the aromatic region of the ^{1}H NMR spectrum. These data were consistent with a dimeric oxidation product (**6**) with a bond between the C-4′ carbon of one steroid moiety and the phenol oxygen of the second steroid moiety. Alternatively, the joining bond might have been between the C-4′ carbon of one steroid moiety and a non-aromatic carbon (e.g. C-9) of the second steroid moiety. However, this latter structural possibility was eliminated by the MS data since four exchangeable protons would have been required but only three were observed (see above and Table 3). Further evidence for the structure **6** was obtained from the COSY and NOESY data which were used to assign the H-6 and H-6′ protons of the product. The two H-6 protons (on the moiety with three aromatic protons) had chemical shifts (2.67 ppm) that were similar to the corresponding protons of ethynylestradiol (2.68 ppm). One of the H-6′ protons (on the moiety with only two aromatic protons) likewise had a similar chemical shift (2.61 ppm) but the second H-6′ proton was more shielded (2.34 ppm). These data were compared with **3a** where all four H-6 and H-6′ protons were shielded (2.2 ppm) by aromatic rings. The data for **6** were thus consistent with the positioning of an oxygen atom between the rings that reduced the shielding effects to only one of the four H-6-type protons.

Product **7** gave a ^{1}H NMR spectrum that showed five signals (two doublets and three singlets) in the aromatic region. These data were consistent with a dimeric oxidation product (**7**) with a bond between the C-2′ carbon of one steroid moiety and the phenol oxygen of the second steroid moiety. Alternatively, the ring-joining bond might have been between the C-2′ carbon of one steroid moiety and a non-aromatic carbon (e.g. C-9) of the second steroid moiety but again this latter possibility was eliminated by the observation of only three exchangeable protons (Table 3). Thus structure **7** was assigned to the product.

3.2. Photodegradation

The photodegradation of ethynylestradiol in acetonitrile in an air atmosphere gave a product distribution that was remarkably similar to the autoxidation product distribution (Fig. 2 and Table 1). HPLC–MS and HPLC–UV were used to confirm the identities of the same predominant products (**2**–**7**).

4. Discussion

The observed autoxidation products probably resulted from free radical pathways that involved peroxyl ($ROO^{\bullet}$) and aryloxyl ($ArO^{\bullet}$) radicals [24–29]. The formation of the 9-hydroperoxide **2** as a predominant product was expected since the 9-position was a tertiary benzylic site [24]. The coupling of aryloxyl radicals to give dimeric products such as **3**–**7** via intermolecular C–C and C–O bond

formation is well known [25–29]. The predominant dimeric products (**3**–**7**) were derived exclusively from ortho–ortho C–C and ortho C–O coupling. Discussions of the coupling process appear elsewhere [25–29].

The photodegradation product mixture was very similar to the autoxidation product mixture and, therefore, some common mechanistic features were likely. Peroxyl radicals were presumably involved since the 9-hydroperoxide (**2**) was observed. Also, aryloxyl radicals were assumed to have been involved in the photochemical formation of the dimeric products **3**–**7** since these types of radicals are known to be involved in the photodegradation of other phenols [30,31].

5. Conclusions

The autoxidation and photodegradation of **1** gave a hydroperoxide and dimeric products that have not been reported previously. The structural assignments were readily achieved with hyphenated on-line techniques without the need to perform time-consuming isolations of the individual compounds.

Acknowledgements

The authors acknowledge Rong Feng and Dawei Xu for helpful discussions.

References

[1] M.L. Cotter, S.D. Levine, R. Mallory, C. Shaw, Tetrahedron Lett. 22 (1978) 1939–1942.
[2] N. Ekiz-Gucer, J. Zappel, J. Reisch, Pharm. Acta Helv. 66 (1) (1991) 2–4.
[3] A.G.J. Sedee, G.M.J. Beijersbergen van Henegouwen, Tetrahedron Lett. 24 (51) (1983) 5779–5780.
[4] N.J.C. Bailey, P. Cooper, S.T. Hadfield, E.M. Lenz, J.C. Lindon, J.K. Nicholson, P.D. Stanley, I.D. Wilson, B. Wright, S.D. Taylor, J. Agric. Food Chem. 48 (2000) 42–46.
[5] A. Lommen, M. Godejohann, D.P. Venema, P.C.H. Hollman, M. Spraul, Anal. Chem. 72 (8) (2000) 1793–1797.
[6] N.J.C. Bailey, P.D. Stanley, S.T. Hadfield, J.C. Lindon, J.K. Nicholson, Rapid Commun. Mass Spectrom. 14 (2000) 679–684.
[7] S.H. Hansen, A.G. Jensen, C. Cornett, I. Bjornsdottir, S. Taylor, B. Wright, I.D. Wilson, Anal. Chem. 71 (22) (1999) 5235–5241.
[8] N. Mistry, A.D. Roberts, G.E. Tranter, P. Francis, I. Barylski, I.M. Ismail, J.K. Nicholson, J.C. Lindon, Anal. Chem. 71 (14) (1999) 2838–2843.
[9] G. Bringmann, K. Messer, M. Wohlfarth, J. Kraus, K. Dumbuya, M. Ruckert, Anal. Chem. 71 (14) (1999) 2678–2686.
[10] S. Strohschein, C. Rentel, T. Lacker, E. Bayer, K. Albert, Anal. Chem. 71 (9) (1999) 1780–1785.
[11] B.C.M. Potts, K.F. Albizati, M.O. Johnson, J.P. James, Magn. Reson. Chem. 37 (6) (1999) 393–400.
[12] S. Strohschein, M. Pursch, K. Albert, J. Pharm. Biomed. Anal. 21 (1999) 669–677.
[13] A.W. Nicholls, J.C. Lindon, R.D. Farrant, J.P. Shockcor, I.D. Wilson, J.K. Nicholson, J. Pharm. Biomed. Anal. 20 (1999) 865–873.
[14] S.X. Peng, B. Borah, R.L.M. Dobson, Y.D. Liu, S. Pikul, J. Pharm. Biomed. Anal. 20 (1999) 75–80.
[15] E. Garo, J.-L. Wolfender, K. Hostettmann, Helv. Chim. Acta 81 (1998) 754–763.
[16] S.D. Taylor, B. Wright, E. Clayton, I.D. Wilson, Rapid Commun. Mass Spectrom. 12 (1998) 1732–1736.
[17] N. Mistry, I.M. Ismail, M.S. Smith, J.K. Nicholson, J.C. Lindon, J. Pharm. Biomed. Anal. 16 (1997) 697–705.
[18] K.I. Burton, J.R. Everett, M.J. Newman, F.S. Pullen, D.S. Richards, A.G. Swanson, J. Pharm. Biomed. Anal. 15 (1997) 1903–1912.
[19] J.K. Roberts, R.J. Smith, J. Chromatogr. A 677 (1994) 385–389.
[20] S.H. Smallcombe, S.L. Patt, P.A. Keifer, J. Magn. Reson. Series A 117 (1995) 295–303.
[21] M. Maumy, J. Rigaudy, Bull. Soc. Chim. Fr. 7–8 (1975) 1879–1882.
[22] P.L. Majumder, M. Basak, Tetrahedron 47 (40) (1991) 8601–8610.
[23] E.L. Eliel, S.H. Wilen, L.N. Mander, Stereochemistry of Organic Compounds, Wiley, New York, 1994, pp. 1142–1150.
[24] K.U. Ingold, Accts. Chem. Res. 2 (1) (1969) 1–9.
[25] D.R. Armstrong, C. Cameron, D.C. Nonhebel, P.G. Perkins, J. Chem. Soc. Perkin Trans. 2 (1983) 587–589.
[26] D.R. Armstrong, C. Cameron, D.C. Nonhebel, P.G. Perkins, J. Chem. Soc. Perkin Trans. 2 (1983) 581–585.
[27] D.R. Armstrong, C. Cameron, D.C. Nonhebel, P.G. Perkins, J. Chem. Soc. Perkin Trans. 2 (1983) 575–579.
[28] D.R. Armstrong, C. Cameron, D.C. Nonhebel, P.G. Perkins, J. Chem. Soc. Perkin Trans. 2 (1983) 569–573.
[29] D.R. Armstrong, C. Cameron, D.C. Nonhebel, P.G. Perkins, J. Chem. Soc. Perkin Trans. 2 (1983) 563–568.
[30] P.R. Levin Jr, I.V. Khudyakov, V.A. Kuz'min, H.J. Hageman, C.R.H.I. de Jonge, J. Chem. Soc. Perkin Trans. 1 (1981) 1237–1239.
[31] J. Audureau, C. Filiol, P. Lemaire, J. Chim. Phys. Phys.-Chim. Bio. 73 (6) (1976) 613–620.